Engineering Notes

ENGINEERING NOTES are short manuscripts describing new developments or important results of a preliminary nature. These Notes cannot exceed 6 manuscript pages and 3 figures; a page of text may be substituted for a figure and vice versa. After informal review by the editors, they may be published within a few months of the date of receipt. Style requirements are the same as for regular contributions (see inside back cover).

Three-Dimensional Transient Heat Conduction in a Multilayer Medium

R.M. Clever*
TRW Systems, Redondo Beach, California
and
A.T. Wassel†
Science Applications, Inc., Hermosa Beach, California

Introduction

In many aerospace applications transient three-dimensional heat conduction calculations are required. Lumped capacitance type computer codes have been used routinely[1,2] which employ either explicit or implicit techniques for solving the governing time-dependent differential equations. These computer codes, although general, have several drawbacks. The explicit codes require a small time step to avoid numerical instability. The implicit codes require inverting large matrices. Both methods can become quite expensive if a large number of nodes are used.

Numerical stability can be achieved in two-dimensional situations by using implicit finite difference techniques, for example, the alternating direction implicit method (ADI). The ADI methods, however, becomes unstable when extended to three-dimensional configurations,[3] and a relation must exist between the time step and spatial grid size in order to ensure stability of the solution.

The purpose of this Note is to present a computational procedure which has been found to be unconditionally stable for three-dimensional situations. The procedure utilizes a time step that can be orders of magnitude larger than that of the fully implicit ADI. A modification to the Douglas scheme is used in solving the governing equtions. Quasilinearization of the boundary conditions and iteration also are used to ensure numerical stability and accuracy with minimum computation expense. The geometry chosen for an application of the method is a three-dimensional Cartesian coordinate system with an arbitrary number of solid layers of dissimilar properties. The numerical example selected is that of the pinwheel radiator base of the thermal control system of an Earth satellite. The base, which is a multi-layer structure, is subjected to nonuniform absorption and emission of radiation at the front surface.

Analysis

The geometry considered is a three-dimensional Cartesian system, with an arbitary number of layers of physically distinct materials in the z coordinate direction, as depicted in Fig. 1. The differential equation of heat conduction is given by

$$\rho c\frac{\partial T}{\partial t}=\frac{\partial}{\partial x}\left(k\frac{\partial T}{\partial x}\right)+\frac{\partial}{\partial y}\left(k\frac{\partial T}{\partial y}\right)+\frac{\partial}{\partial z}\left(k\frac{\partial T}{\partial z}\right) \tag{1}$$

where $\rho c, k$, and T are the density, specific heat, thermal conductivity, and temperature, respectively. The variable t is time and x, y, and z are the three coordinate directions. Several boundary conditions are possible at the external surfaces, such as

$$-k\partial T/\partial n=q(t,T),\ \partial T/\partial n=q(t),\ \text{or}\ T=T(t) \tag{2}$$

The solution to Eq. (1), with appropriate boundary conditions, was obtained using a modification to the Douglas[4,5] scheme. The manner in which the scheme was used to provide an unconditionally stable algorithm is given by the following equations which are solved in succession.

x direction loop

$$(T^1-T^*)/\delta t=0.5\left[\delta_x^2(T^1+T^*)+\delta_y^2(\hat{T}+T^*)+\delta_z^2(\hat{T}+T^*)\right] \tag{3}$$

y direction loop

$$(T^2-T^*)/\delta t=0.5\left[\delta_x^2(T^1+T^*)+\delta_y^2(T^2+T^*)+\delta_z^2(\hat{T}+T^*)\right] \tag{4}$$

z direction loop

$$(\hat{T}-T^*)/\delta t=0.5\left[\delta_x^2(T^1+T^*)+\delta_y^2(T^2+T^*)+\delta_z^2(\hat{T}+T^*)\right] \tag{5}$$

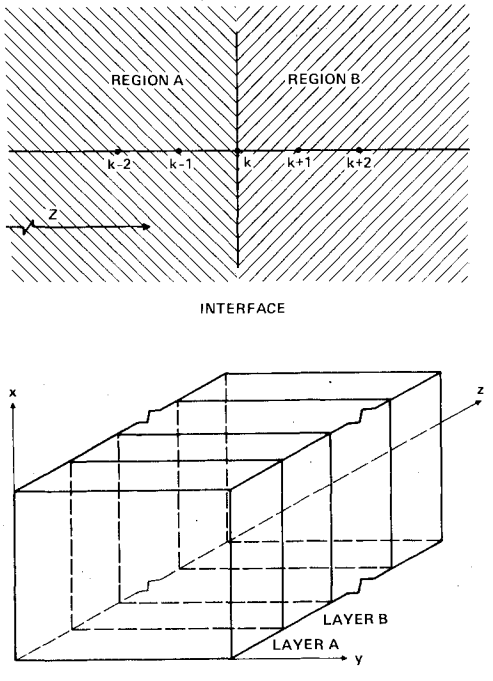

Fig. 1 Geometry and coordinate system.

Received Nov. 23, 1983; revision received March 17, 1984.

*Member Technical Staff.
†Manager. Member AIAA.

Here the four intermediate temperatures are: T^* = temperature at the previous timestep, T^1 = x-direction temperature, T^2 = y-direction temperature, and $\hat{T}$ = z-direction and previous iterate temperature. The x-, y-, and z-direction components of the Laplacian operator are represented by δ_x^2, δ_y^2, and δ_z^2, respectively.

The finite difference analogue of Eq. (1) was formulated in terms of second-order correct spatial derivative expressions of the interior node points with full matching conditions at the interface between layers. Linearized boundary condition expressions and an iterative scheme were also used.

The finite difference equations for the interior node points are obtained in a straightforward manner and can be written as follows:

$$\begin{aligned} T_{ijk} &= T^*_{ijk} + A_x(T_{i+1,j,k} + T^*_{i+1,j,k}) + B_x(T_{ijk} + T^*_{ijk}) \\ &+ C_x(T_{i-1,j,k} + T^*_{i-1,i,k}) + A_y(T_{i,j+1,k} + T^*_{i,j+1,k}) \\ &+ B_y(T_{ijk} + T^*_{ijk}) + C_y(T_{i,j-1,k} + T^*_{i,j-1,k}) \\ &+ A_z(T_{i,j,k+1} + T^*_{i,j,k+1}) + B_z(T_{ijk} + T^*_{ijk}) \\ &+ C_z(T_{i,j,k-1} + T^*_{i,j,k-1}) \end{aligned} \tag{6}$$

where A, B, and C are the finite difference coefficients and (i, j, and k) denote a point in the medium. The temperature T on the right side of Eq. (6) assumes the quantities T^1, T^2, and T, respectively, depending on the alternating direction of sweep.

The matching conditions for the interface node points follow from a Taylor series expansion of the temperature in terms of temperature values at, and adjacent to, the interface. Substitution of these expansions into the differential equations for adjacent regions provides the necessary algebraic conditions. If A and B denote two arbitrary adjacent regions (see Fig. 1), a Taylor series expansion in regions A and B yields the adjacent node point values

$$T_{k-1} = T_k - (\delta z)_A \left(\frac{\partial T}{\partial z}\right)_A + \frac{(\delta z)_A^2}{2}\left(\frac{\partial^2 T}{\partial z^2}\right)_A \tag{7a}$$

$$T_{k+1} = T_k + (\delta z)_B \left(\frac{\partial T}{\partial z}\right)_B + \frac{(\delta z)_B^2}{2}\left(\frac{\partial^2 T}{\partial z^2}\right)_B \tag{7b}$$

where k denotes the interface node point. Substituting Eqs. (7a) and (7b) into the heat conduction equations of regions A and B, and rearranging results in

$$\begin{aligned} k_A\Gamma_A\Gamma_B\left(\frac{\partial T}{\partial z}\right)_A &= k_A\Gamma_B\left[(\rho c)_A\frac{\partial T}{\partial t}\right. \\ &\left. - L_A(k_A, T) - \frac{2K_A}{(\delta z)_A^2}(T_{k-1} - T_k)\right] \end{aligned} \tag{8a}$$

$$\begin{aligned} k_B\Gamma_A\Gamma_B\left(\frac{\partial T}{\partial z}\right)_B &= -k_B\Gamma_A\left[(\rho c)_B\frac{\partial T}{\partial t}\right. \\ &\left. - L_B(k_B, T) - \frac{2k_B}{(\delta z)_B^2}(T_{k+1} - T_k)\right] \end{aligned} \tag{8b}$$

where

$$\Gamma_A = \left(\frac{2k}{\delta z}\right)_A + \left(\frac{\partial k}{\partial z}\right)_A \qquad \Gamma_B = \left(\frac{2k}{\delta z}\right)_B - \left(\frac{\partial k}{\partial z}\right)_B \tag{9}$$

$$L_{A,B} = \frac{\partial}{\partial x}\left(k\frac{\partial T}{\partial x}\right)_{A,B} + \frac{\partial}{\partial y}\left(k\frac{\partial T}{\partial y}\right)_{A,B} \tag{10}$$

The heat flux matching conditions at the interface $k_A(\partial T/\partial z)_A = k_B(\partial T/\partial z)_B$ provides the necessary closure condition. After substitution and normalization, the governing equation at the interface of dissimilar materials is obtained

$$\begin{aligned} [\lambda_{AB}(\rho c)_A + \lambda_{AB}(\rho c)_B]\frac{\partial T}{\partial t} &= \frac{\partial}{\partial x}\left(k_{AB}\frac{\partial T}{\partial x}\right) \\ &+ \frac{\partial}{\partial y}\left(k_{AB}\frac{\partial T}{\partial y}\right) + \frac{2k_A\lambda_{AB}}{(\delta z)_A^2}(T_{k-1} - T_k) + \frac{2k_B\lambda_{BA}}{(\delta z)_B^2}(T_{k+1} - T_k) \end{aligned} \tag{11}$$

$$\lambda_{AB} = \frac{k_A\Gamma_B}{k_A\Gamma_B + k_B\Gamma_A}, \qquad \lambda_{BA} = \frac{k_B\Gamma_A}{k_A\Gamma_B + k_B\Gamma_A} \tag{12}$$

and $k_{AB} = \lambda_{AB}K_A + \lambda_{BA}k_B$. All derivatives of k_{AB} are to be taken with both λ_{AB} and λ_{BA} held constant. The interface finite difference coefficients A_x, B_x, C_x, etc., can now be found from Eq. (11), similar to the interior node points.

The boundary condition algorithm at each of the six faces is obtained as follows. A fully linearized algorithm for the surface heat flux is derived from a Taylor series expansion of q with respect to a previous time step

$$q = q^*\{T^*\} + \frac{dq}{dT}\{T^*\}(T - T^*) \tag{13}$$

which, if written in the finite difference form (at the $z=0$ face, for example), yields (the subscript ij is dropped for ease of reading):

$$T_1 = T_3 + q_\beta(2\delta z/k_2) + q_\alpha(2\delta z/k_2)T_2 \tag{14}$$

where

$$q_\alpha = \frac{dq}{dT}\{T_2^*\} \quad \text{and} \quad q_\beta = q^*\{T_2^*\} - \frac{dq}{dT}\{T_2^*\}T_2^* \tag{15}$$

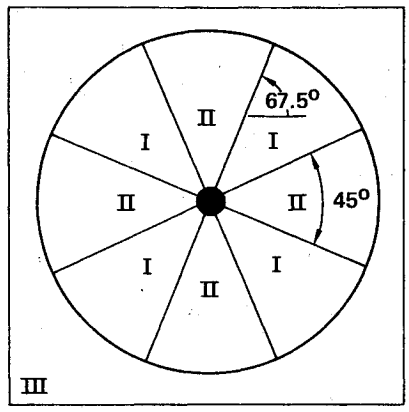

Pinwheel Radiator Base (Aluminized Teflon (I), Aluminized Kapton (II) and Multilayer Insulation (III))

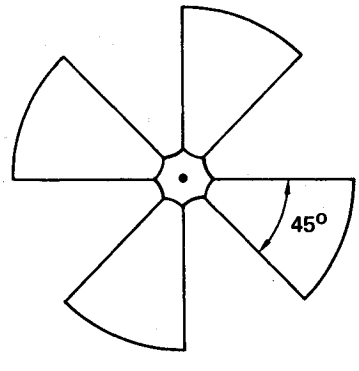

Pinwheel Radiator Louver

Fig. 2 Pinwheel radiator, schematics.

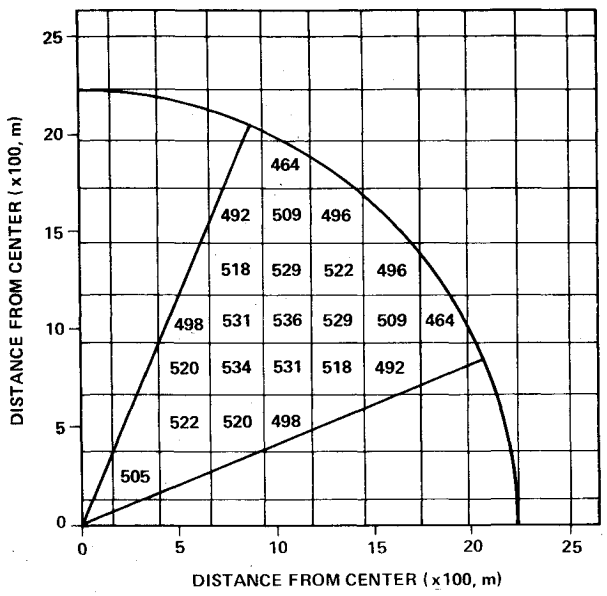

Fig. 3a Frontface temperature distribution after 60 s exposure, $\theta_b = 67.5$ deg and $\bar{q} = 20{,}000$ W/m^2.

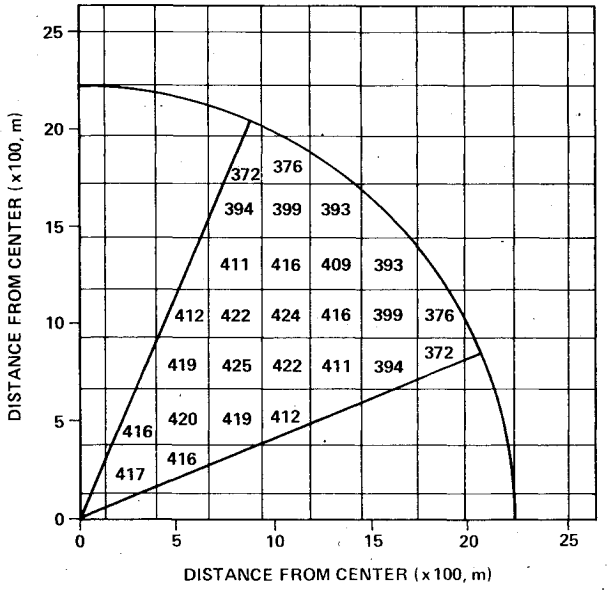

Fig. 3b Backface temperature distribution after 60 s exposure, $\theta_b = 67.5$ deg and $\bar{q} = 20{,}000$ W/m^2.

and T_I is the temperature at the image point of node point 3. The finite difference equation of the surface nodes ($z=0$, $k=2$) is then used to eliminate T_I from Eq. (14) and the solution algorithm is now complete. A similar manipulation is performed for the other faces.

Application

Several validation cases were performed by comparing the numerical solutions of selected Cartesian geometries to analytic solutions[6] in order to test both the accuracy and stability of the numerical scheme. Also, the procedure was compared against the fully implicit three-dimensional ADI scheme.[3] The time step of the proposed method was in some cases three orders of magnitude larger than that required by the fully implicit ADI.

The pinwheel radiator is a satellite thermal control device. it is a multilayer component which requires a fully three-dimensional analysis to determine its transient thermal

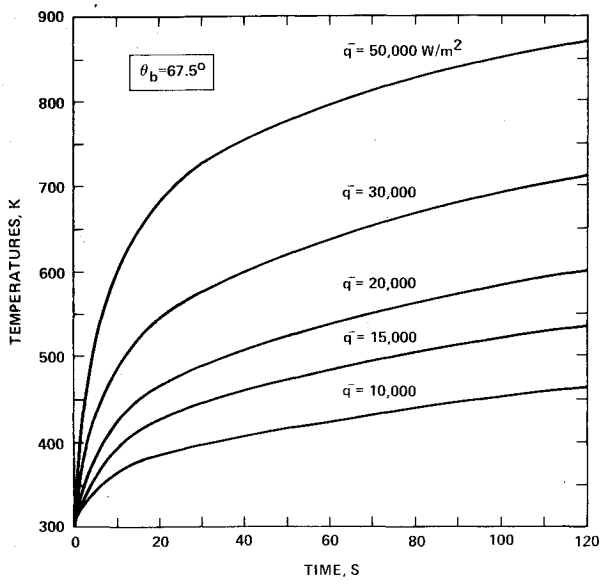

Fig. 4a Transient maximum frontface temperature, $\theta_b = 67.5$ deg.

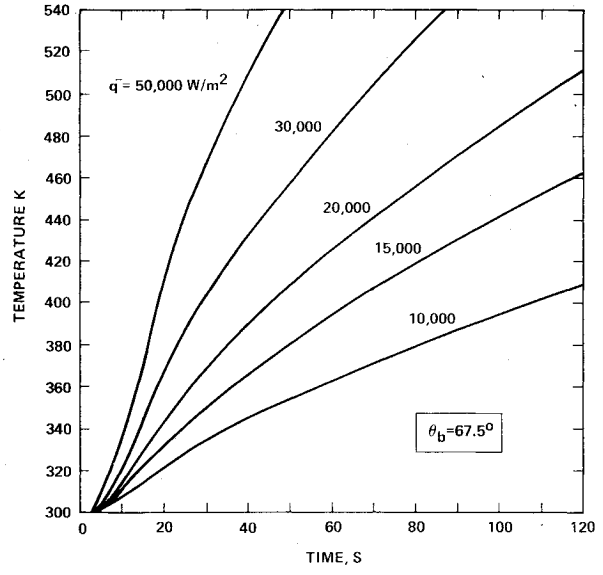

Fig. 4b Transient maximum backface temperature, $\theta_b = 67.5$ deg.

response. It consists of two physically distinct parts; the base and a rotating louver blade, as shown in Fig. 2. The base is made out of an aluminum honeycomb which is sandwiched between two aluminum face sheets. Alternating 45 deg segments of the exposed circular radiator portion of the base have aluminized kapton or teflon outer layers glued on the front face sheet. These segments are beneath the blade. The dissimilar absorptive and emissive properties of the materials in conjunction with blade rotation provide the thermal control. The rest of the base front surface that is not shielded by the louver blade is covered with a multilayer insulation blanket which is placed on the base to allow very low heat leakage. The base is composed of seven layers that are in thermal contact. These layers are kapton or teflon, adhesive, aluminum substrate, adhesive, honeycomb, adhesive, and aluminum substrate. The honeycomb filling is treated as a layer with an in-depth effective thermal conductivity which is based on the void fraction of the honeycomb structure.

The thermal response of the base structure to a uniform front face irradiative flux was determined as follows. As a result of the varying radiative properties of the front surface, the net flux applied to the various zones depends on the front

face material exposed. The net absorbed flux is given by $q_{net} = \alpha\bar{q} - \epsilon\sigma T^4$. The absorptivity α and emissivity ϵ were taken as follows: for region I (teflon) $\alpha_T = 0.9$ and $\epsilon_T = 0.85$, for region II (kapton) $\alpha_k = 0.06$ and $\epsilon_k = 0.06$, and for region III or portions of regions I and II that are shielded by the louverblade, α and ϵ were assumed to be small in order to effect an adiabatic boundary condition. The irradiation flux, $\bar{q}$ was varied as a parameter in the calculations. The front face was effectively subjected to a highly three-dimensional heat flux caused by the different localized net heat absorption. Adiabatic boundaries were assumed for the other five faces of the base structure.

Calculations were performed to predict the thermal response of the base structure subject to front face irradiation. The incident flux was varied up to 50,000 W/m^2.

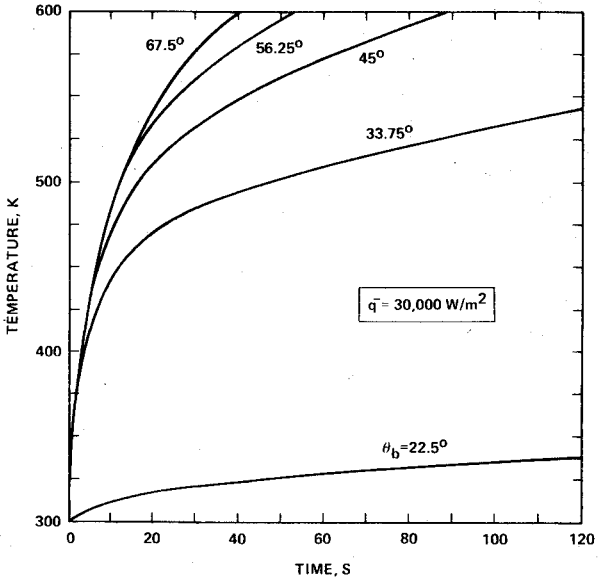

Fig. 5a Transient maximum frontface temperature, $\bar{q} = 30{,}000$ W/m^2.

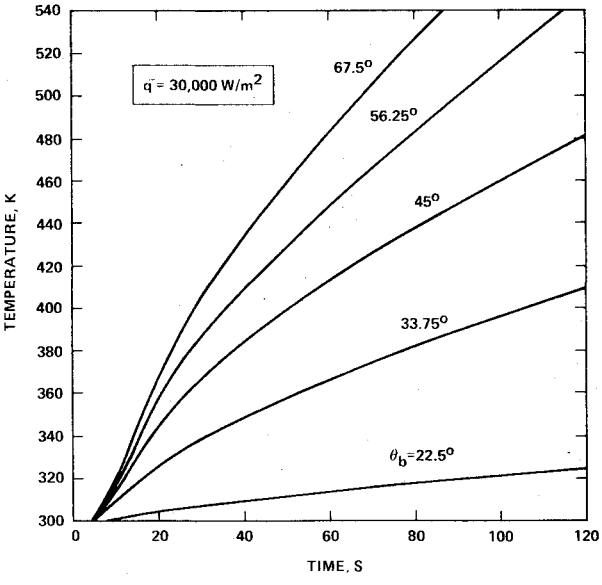

Fig. 5b Transient maximum backface temperature, $\bar{q} = 30{,}000$ W/m^2.

The blade setting was also varied as a parameter in the following fashion: $\theta_b = 22.5$ deg (all aluminized kapton exposed), $\theta_b = 45$ deg (50% teflon and 50% aluminized kapton exposed) and $\theta_b = 67.5$ deg (all teflon exposed). The base was divided into typically a 20×20 macro-nodal grid in the x-y plane, and each layer in depth (z direction) was divided into several slices (up to four). Each micro-grid cell was then divided into a 20×20 micro-grid which was used to calculate the percentage of the macro-grid surface area that was covered by kapton or teflon, or insulated depending on the base setting. The net incident flux of irradiation was then calculated accordingly. The time step size, δt, used in the calculations was 0.5 s. A calculation was done using a smaller value of δt, 0.1. The results differed from those with $\delta t = 0.5$ s by less than 1%. An initial temperature of 300 K was assumed for all the layers.

Typical results are shown in Figs. 3a and 3b, where the temperature maps are shown for the front face (Fig. 3a) and back face (Fig. 3b) after 60 s of exposure. The irradiation flux was 20,000 W/m^2 and the blade angle was 67.5 deg. The temperature distributions show the highly three-dimensional response due to the highly three-dimensional nature of the net absorbed flux. At 30 s, the maximum front and back face temperatures were 489 K and 370 K, while at 60 s the corresponding temperatures were 536 K and 425 K. The location of the maximum temperature is at the center of the teflon surface. The results also show that as the heat is transferred in depth, the nonuniformity in the temperature distribution is somewhat smoothed out.

Figures 4a and 4b are plots of the maximum front (Fig. 4a) and back (Fig. 4b) face temperatures for various levels of irradiation with a blade angle of 67.5 deg. Note that for short values of time the front face maximum temperature rise varies quite strongly, approximately linearly with flux. For larger values of time, the temperature rise is somewhat less than linear owing to the nonlinearity of the energy reradiated. The back face temperature rise, on the other hand, varies almost linearly with flux for a much longer period of time.

We see in Figs. 5a and 5b the very strong dependence of temperature rise on blade angle, for a flux of 30,000 W/m^2. Merely changing the blade angle from 22.5 to 33.75 deg, one-fourth of the high absorptivity material exposed, shows an increase of a factor of six in maximum front face temperature. Complete exposure of the high-absorptivity front face results in another factor of two increase in temperature rise. This also indicates the importance of lateral conduction for the intermediate blade angles.

References

[1] Smith, J.P., "SINDA User's Manual," Redondo Beach, Calif., TRW 14690-H001-R0-00, April 1971.

[2] O'Neill, R.F., et al., "Variable Boundary Heat Conduction Program," *General Dynamics,* GDC-87D67-004 A (NTIS N69-29705), Sept 1968.

[3] Carnahan, B., Luther, H.A., and Wilkes, J.O., *Applied Numerical Methods,* John Wiley & Sons, Inc., New York, 1969, pp. 451-453.

[4] Douglas, J., "Iterative Methods for Three Space Variables," *Numerische Mathematic,* Vol. 4, 1962, pp. 41-63.

[5] Douglas, J. and Gunn, J.E., "A General Formulation Alternating Direction Methods, Part I, Parabolic and Hyperbolic Problems," *Numerische Mathematic,* Vol. 6, 1964, pp. 428-453.

[6] Carslaw, H.S. and Jaeger, J.C., *Conduction of Heat in Solids,* 2nd ed., Oxford University Press, 1959.